ARTICLE

Check for updates

Journal of
Sensor Science and Technology

The Korean Sensors Society

Piezoelectric Strain Characteristics of $BiFeO_3$-$BaTiO_3$ Ceramics around the MPB Composition

Ye-Rok Choi[1], Chae-Il Cheon[1], and Ki-Woong Chae[1,+]

[1]*Department of Electronic Materials and Engineering, Hoseo University, Asan 31499, Republic of Korea*

Cite This: *J. Sens. Sci. Technol. Vol. 35, No. 3 (2026) 216-224*

https://doi.org/10.46670/JSST.2026.35.3.216

ABSTRACT: The crystal structure, phase transition behavior, ferroelectric P-E and S-E hysteresis characteristics, and piezoelectric properties were investigated in (1-x)$BiFeO_3$-x$BaTiO_3$ (BF-BT) solid-solution ceramics ($0.2 \leq x \leq 0.5$). The ferroelectric rhombohedral phase transformed into a relaxor pseudo-cubic phase as the BT mole fraction increased from 0.2 to 0.5. The two phases coexisted in the composition range of 0.25–0.4, and the fraction of the pseudo-cubic phase increased with an increasing BT mole fraction. The 0.7BF-0.3BT sample, located in the MPB composition region, exhibited moderate piezoelectric properties, including a piezoelectric charge constant (d_{33}) of 178 pC/N and an electromechanical coupling factor (k_p) of 0.357, along with a high Curie temperature (T_c) of 516°C, suggesting strong potential for high-temperature piezoelectric sensor applications. The ferroelectric P-E and S-E hysteresis curves of the x = 0.2–0.3 compositions showed unsaturated profiles due to their high coercive fields, while the x = 0.35 composition exhibited well-saturated P-E and S-E hysteresis curves, as well as the largest polarization and strain, owing to its low coercive field and the MPB effect. As the BT mole fraction increased to 0.4 or higher, polarization and strain decreased continuously because of the increased fraction of the ergodic relaxor phase. The 0.6BF-0.4BT sample showed a large unipolar strain of 0.308% and a high piezoelectric strain constant (d_{33}*) of 513 pC/N with a moderate strain hysteresis of 0.25%, features that are favorable for piezoelectric actuator applications.

KEYWORDS: *$BiFeO_3$-$BaTiO_3$, Ceramics, Piezoelectric, Strain*

1. INTRODUCTION

Piezoelectric materials produce mechanical deformation when an electric field is applied and exhibit electric polarization when mechanical stress is applied. These piezoelectric materials can provide fast and precise displacements through electromechanical energy conversion, and thus are used in actuators in various fields such as micro-motion devices, microscope lenses, and fuel injectors [1]. Currently, Pb-based piezoelectric single-crystal and polycrystalline ceramics, such as $Pb(Zr_{0.47}Ti_{0.53})O_3$ and $Pb(Ni_{1/3}Nb_{2/3})O_3$-$PbTiO_3$-$PbZrO_3$, are widely used in piezoelectric sensors and actuators due to their excellent piezoelectric properties and large strains [2-6]. However, these materials are harmful to the human body due to the toxicity of lead (Pb). Therefore, global environmental regulations such as RoHS and WEEE have been implemented, and eco-friendly lead-free piezoelectric materials have been developed to replace Pb-based materials [7]. To date, the lead-free piezoelectric ceramics exhibiting the most outstanding piezoelectric properties include $(Bi_{0.5}Na_{0.5})TiO_3$ (BNT), $(K_{0.5}Na_{0.5})NbO_3$ (KNN), and $Ba(Ti_{0.8}Zr_{0.2})O_3$-$(Ba_{0.7}Ca_{0.3})TiO_3$. However, these materials have disadvantages such as high sintering temperatures of 1100–1500°C and low phase transition temperatures of 200°C or less [5-7]. Meanwhile, $BiFeO_3$-$BaTiO_3$ (BF-BT) solid solution ceramics have received much attention as eco-friendly high-temperature piezoelectric materials because they exhibit a high Curie temperature and moderate piezoelectric properties [8,9]. As the BT mole fraction (x) increases in (1-x)BF-xBT solid solution ceramics, the structure changes from a ferroelectric rhombohedral phase to a relaxor ferroelectric pseudo-cubic phase around x = 0.3, and the two phases coexist in the morphotropic phase boundary (MPB) region [10-12]. It has been reported that BF-BT ceramics show excellent ferroelectricity and piezoelectric properties in the MPB composition region, and exhibit maximum piezoelectric strain

+Corresponding author: chaekw@hoseo.edu
Received : Apr. 10, 2026, Accepted : Apr. 17, 2026

in the pseudo-cubic phase at a BT mole fraction slightly higher than that of the MPB composition [10,12]. Various studies have been conducted to adjust the composition ratio in BF-BT ceramics to obtain maximum strain and low strain hysteresis [8,13-15]. J. Chen et al. obtained excellent piezoelectric strain characteristics such as a maximum strain of 0.38% and a piezoelectric strain constant (d_{33}*) of 633 pm/V, by applying an electric field of 6 kV/mm to a 0.64BF-0.36BT ceramic with the cubic relaxor phase. However, the strain hysteresis of this composition showed a large value of 47% [16]. C. Li et al. reported that the ferroelectric and relaxor phases coexist in the composition range of $0.25 \leq x \leq 0.45$ for (1-x)BF-xBT ceramics, and the size of the large ferroelectric domains gradually decreases as the BT content increases [17]. Furthermore, they reported that a typical relaxor-type strain-electric field (S-E) hysteresis curve with almost no negative strain was observed in compositions with a large relaxor phase fraction ($x \geq 0.35$) and nano-domains [17]. Meanwhile, B. Xun et al. obtained a moderate strain (0.21%) and piezoelectric charge constant (d_{33} = 405 pm/V), together with excellent strain hysteresis (17%) in 0.65BF-0.35BT ceramics. They claimed that these characteristics were due to the fine control of the composition ratio to obtain a polarization structure where ferroelectric domains and polar nano-regions (PNRs) coexist [10]. These reports show that the composition near the MPB region of BF-BT ceramics has a significant effect on the strain. However, the experimental results and interpretations regarding the change in strain according to the composition ratio are inconsistent among these reports [14]. Meanwhile, several reports have also improved strain characteristics by forming solid solutions with other perovskite compounds, such as $BiFeO_3$-$BaTiO_3$-$Bi(Mg_{2/3}Nb_{1/3})O_3$ and $BiFeO_3$-$BaTiO_3$-$(Ba_{0.6}Sr_{0.4})TiO_3$, or by doping with Sm_2O_3, Nb_2O_5, and other oxides [8,14,18-20].

In this work, the piezoelectric strain characteristics were investigated over a wide composition range ($0.2 \leq x \leq 0.5$) spanning the ferroelectric phase, MPB, and relaxor phase in (1-x)BF-xBT binary solid solution ceramics. The crystal structures were verified through X-ray diffraction analysis, and the ferroelectric and relaxor phase transition behaviors were investigated based on the change in dielectric constant with temperature. In addition, the switching characteristics of the ferroelectric domains were analyzed by measuring the ferroelectric polarization-electric field (P-E) and strain-electric field (S-E) hysteresis characteristics. The change in strain with composition is explained, and the composition showing the optimal piezoelectric strain characteristics is presented for BF-BT ceramics.

2. EXPERIMENTAL

BF-BT ceramics were fabricated using a solid-state synthesis method. The raw powders were Bi_2O_3 (≥ 99.9%, Sigma-Aldrich), Fe_2O_3 (≥ 99%, Sigma-Aldrich), $BaCO_3$ (≥ 99%, Sigma-Aldrich), and TiO_2 (≥ 99.9%, High Purity Chemicals). The raw powders were loaded into a plastic bottle with stabilized zirconia balls and ethanol, and then mixed for 24 hours by ball milling. The slurry was dried on a hot plate while stirring, and the dried powder was calcined at temperatures of 900–1000°C for 2 hours. To improve insulation resistance, 0.1–0.2 mol% of MnO_2 was added to the calcined powder, and the mixed powder was ball-milled again. The mixed slurry was dried, granulated, and pressed in a disk-shaped mold by applying a uniaxial pressure of 100 MPa. The pressed samples were sintered at temperatures of 940–1050°C for 3 hours. Silver paste was applied to the surface of the sintered specimens and sintered at 800°C for 15 minutes, after which the samples were removed and quenched in air.

The crystal structure of the sintered samples was characterized using X-ray diffraction (XRD; XRD-6100, Shimadzu), and the crystal structure was analyzed in detail using the Rietveld refinement method with the FullProf program. The dielectric constant and dielectric loss were measured using an impedance analyzer (4294A, Agilent, USA), and the temperature dependence of the dielectric constant was measured as the temperature was increased from room temperature to 600°C. The ferroelectric polarization-electric field (P-E) hysteresis curve was measured using a ferroelectric tester (RT66-C, Radiant, USA) and a high-voltage amplifier (10/10B-HS, TREK). A 0.1 Hz bipolar or unipolar triangular wave was applied to the specimen using a function generator (33220A, Agilent, USA) and a high-voltage amplifier for strain measurement. The strain generated by the electric field was measured with a linear variable differential transformer (LVDT) sensor and a displacement measurement device (TESA TT60, Electronic Length Measuring Equipment, Switzerland). The piezoelectric strain constant (d_{33}* = S_{max} / E_{max}) was obtained by dividing the maximum unipolar strain (S_{max}) by the applied maximum electric field (E_{max}). The samples were placed in silicone oil and poled under a DC electric field of 3 kV/mm for 30 minutes at 120°C. The piezoelectric charge constant (d_{33}) was measured using a d_{33} meter (YE2730A, APC International Ltd.), and the electromechanical coupling factor (k_p) was measured by the resonance-antiresonance method using an impedance analyzer.

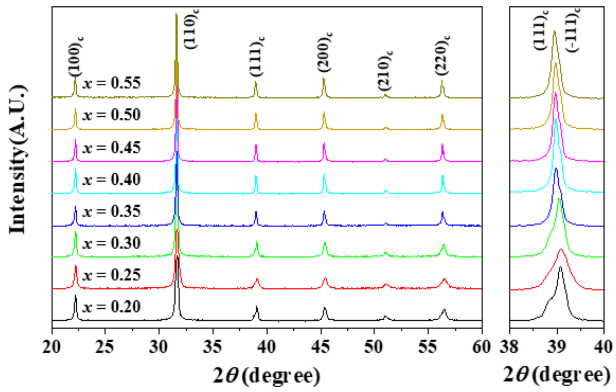

Fig. 1. XRD patterns of (1-*x*)BF-*x*BT ceramics.

3. RESULTS AND DISCUSSIONS

Fig. 1 shows the XRD patterns of the sintered (1-*x*)BF-xBT ceramics, with the Miller indices indicated based on the cubic structure. As shown in Fig. 1, the perovskite solid solution was synthesized without any impurity phases in the samples of all compositions. The right side of Fig. 1 provides a detailed view of the 2θ = 38-40° range, confirming the splitting of the diffraction peaks for the {111} planes arising from the distortion of the rhombohedral structure. Fig. 1 shows that the diffraction peaks for the (111) and ($11\bar{1}$) planes are separated in the composition range where the BT mole fraction (*x*) is 0.2–0.3, but the diffraction peaks merge into one as *x* increases to 0.35 or higher. As reported in previous papers, this indicates that the crystal structure changes from rhombohedral to pseudo-cubic as the BT mole fraction increases [10-12].

To investigate the change in the crystal structure of (1-*x*)BF-*x*BT ceramics according to composition in detail, Rietveld refinement analysis was performed, and the results are summarized in Table 1. Table 1 shows that the rhombohedral ($R3c$) phase and the pseudo-cubic ($Pm\bar{3}m$) phase coexist in the composition range where the BT mole fraction is 0.25–0.4.

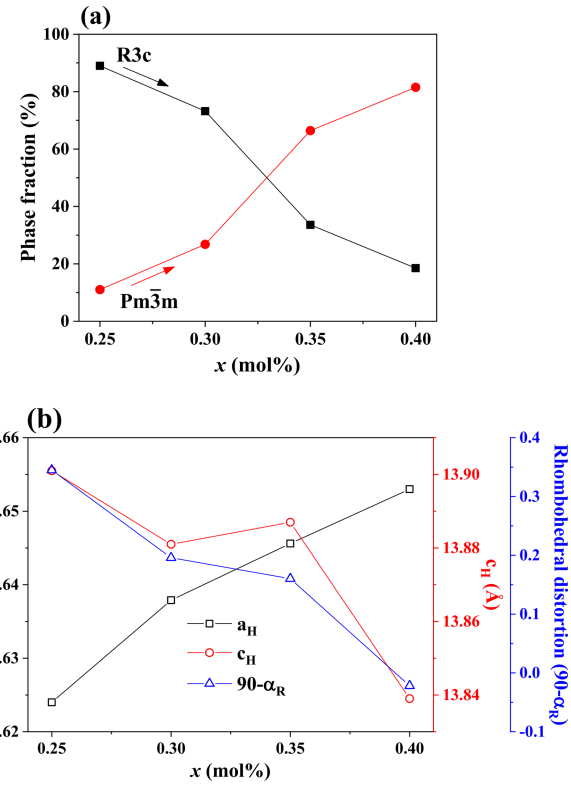

Fig. 2. Changes in (a) phase fractions and (b) lattice constants with the BT mole fraction (*x*) in (1-*x*)BF-*x*BT ceramics.

The changes in the ratio of the two phases and the lattice constants of the rhombohedral phase with increasing BT mole fraction are shown in Fig. 2(a) and (b). As shown in Fig. 2(a), when the BT mole fraction was 0.25, the fraction of the rhombohedral phase was 0.89, representing the dominant phase; however, as *x* increased, the fraction of the rhombohedral phase gradually decreased, while the fraction of the pseudo-cubic phase continued to increase, becoming the dominant phase at *x* = 0.4. Furthermore, Fig. 2(b) illustrates that as the BT mole fraction increases, the lattice constant 'a' of

Table 1. Rietveld refinement results for (1-*x*)BF-*x*BT ceramics.

Composition	phase (SG)	fraction	lattice parameters a (Å)	b (Å)	c (Å)	R factors R_p	R_{wp}	R_{exp}	R_b	R_f
0.25 BT	R3c	89.0	5.6240(3)	5.6240(3)	13.901(1)	2.76	3.50	2.76	7.45	7.04
	$Pm\bar{3}m$	11.0	3.9772(8)	3.9772(8)	3.9772(8)				5.61	4.41
0.30 BT	R3c	73.2	5.6379(6)	5.6379(6)	13.881(13)	2.75	3.47	2.86	8.64	8.35
	$Pm\bar{3}m$	26.8	3.9867(5)	3.9867(5)	3.9867(5)				7.73	6.31
0.35 BT	R3c	33.6	5.6456(7)	5.6456(7)	13.887(20)	3.57	4.57	3.13	11.4	9.79
	$Pm\bar{3}m$	66.4	3.9935(1)	3.9935(1)	3.9935(1)				10.8	7.42
0.40 BT	R3c	18.5	5.65304	5.65304	13.839(26)	3.17	4.06	3.06	12.6	15.7
	$Pm\bar{3}m$	81.5	3.9963	3.9963	3.9963				11.0	11.3

the rhombohedral phase increases and 'c' decreases, indicating a reduction in the rhombohedral distortion (90^{o}-α). The results in Fig. 2 are consistent with previous reports showing that as the BT mole fraction increases in the MPB region of (1-*x*)BF-*x*BT ceramics, the fraction of the pseudo-cubic phase increases and the distortion of the rhombohedral phase decreases [17,21].

Figs. 3(a) and (b) show the change in dielectric constant with increasing temperature for the x = 0.3 and 0.35 compositions of (1-*x*)BF-*x*BT ceramics. The x = 0.3 sample shows a sharp dielectric constant peak at 516^{o}C regardless of the measurement frequency, which corresponds to the Curie temperature (T_C) for the transition from the ferroelectric phase to the paraelectric phase. The T_C is much higher than that of other lead-free piezoelectric ceramics such as BNT-BT and KNN. On the other hand, the x = 0.35 sample shows a strong frequency dependence, in which the peak of the dielectric constant moves toward lower temperatures as the measurement frequency decreases, and the dielectric constant peak shows a much broader shape than that of the x = 0.3 specimen. This temperature dependence of the dielectric constant is known as typical phase transition behavior observed in relaxor ferroelectrics [12-22]. Furthermore, samples with a BT mole fraction of 0.3 or less showed a sharp dielectric constant peak without frequency dependence, as shown in Fig. 3(a), while samples with x = 0.35 or higher showed frequency dependence similar to Fig. 3(b). These results are consistent with the findings in Table 1 and Fig. 2, which show that the ferroelectric rhombohedral phase is dominant when the BT mole fraction is 0.3 or less, and the pseudo-cubic phase is dominant when x is 0.35 or higher; these results suggest that the pseudo-cubic phase is a relaxor ferroelectric phase as previously reported. Fig. 3(c) shows the temperature dependence of the dielectric constant for samples with x = 0.35 or higher. The figure shows that as x increases, the temperature at which the dielectric constant is maximum (T_{max}) gradually moves toward lower temperatures, the peak of the dielectric constant gradually becomes broader, and the maximum value of the dielectric constant at T_{max} gradually decreases. The phase transition of the relaxor ferroelectric phase and the resulting change in the dielectric constant are generally explained as follows [22]. When the temperature decreases below the high-temperature paraelectric state, polar nano-regions (PNRs) begin to form below the Burns temperature (T_B). The polarization of the PNRs maintains a dynamic state due to thermal fluctuations, thereby contributing to the increase in the dielectric constant. As the temperature decreases, the number and average size of PNRs increase, showing a maximum value of the dielectric constant; due to the size distribution of PNRs, a difference in the dielectric

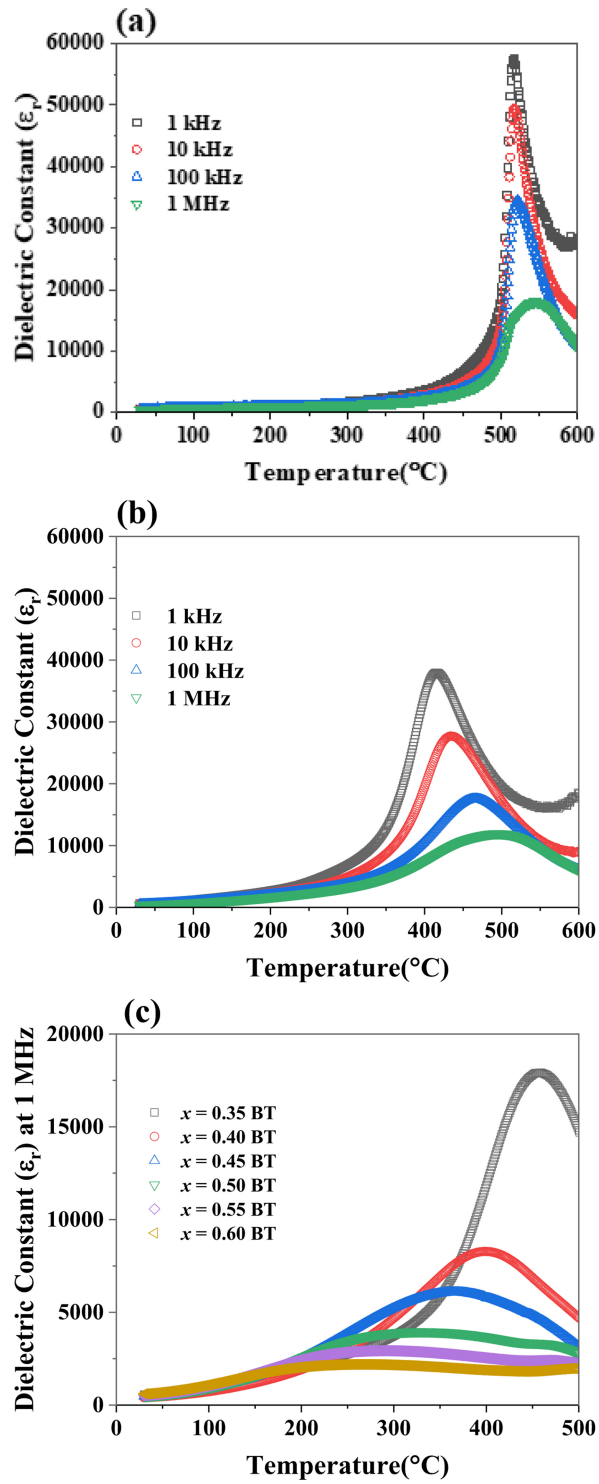

Fig. 3. Temperature-dependent dielectric constants of (1-*x*)BF-*x*BT ceramics at (a) x = 0.3 and (b) x = 0.35, and (c) the dielectric peaks at x ≥ 0.35.

constant according to the measurement frequency, i.e., dielectric dispersion, appears. When the temperature continues to decrease below T_{max}, the size of the PNRs continues to grow and the dynamic characteristics weaken, so the degree of

contribution to the dielectric constant gradually decreases; the temperature at which the dynamic characteristics of the PNRs disappear is called the freezing temperature (T_f). In the temperature range between T_B and T_f, the arrangement of PNRs can change reversibly; therefore, when an external electric field is applied, the polarization is temporarily arranged, but when the electric field is removed, it returns to a disordered state. This thermally reversible state is called an ergodic relaxor. Furthermore, the state below T_f where the dynamic characteristics of the PNRs have disappeared is called a non-ergodic relaxor; in this case, if a large electric field is applied, it irreversibly changes to a ferroelectric phase. In Fig. 3(c), the decrease in T_{max} as the BT mole fraction (x) increases means that the relaxor phase transition gradually moves toward lower temperatures, and the decrease in the dielectric constant peak value is thought to be because the number of PNRs decreased, reducing the degree of contribution to the dielectric constant. Fig. 4 shows the changes in (a) dielectric constant and dielectric loss (tan δ), and (b) electromechanical coupling factor (k_p) and piezoelectric charge constant (d_{33}) with

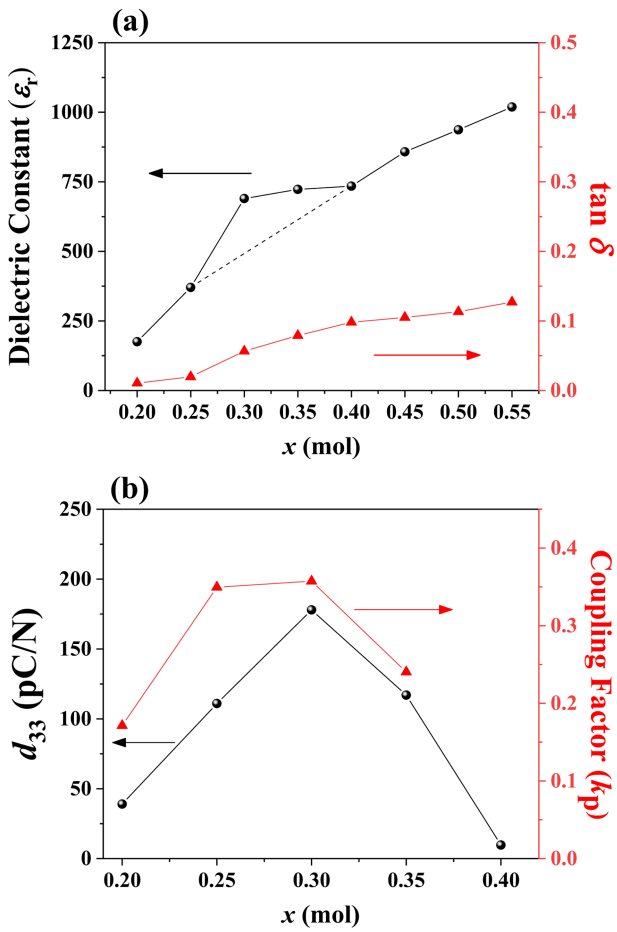

Fig. 4. Changes in (a) dielectric constant and loss and (b) piezoelectric properties (k_p, d_{33}) with the increase of BT mole fraction (x) in (1-x)BF-xBT ceramics.

increasing BT mole fraction of (1-x)BF-xBT ceramics. As shown in Fig. 4(a), the dielectric constant increased as the BT mole fraction increased because the dielectric constant of BT is much larger than that of BF. Furthermore, in the MPB composition region ($0.25 < x < 0.4$), the dielectric constant increased more than the linear increase (indicated by the dotted line in Fig. 4(a)) with increasing x, which is thought to be due to the MPB effect. The electromechanical coupling factor (k_p) and the piezoelectric charge constant (d_{33}) showed large values in the composition range with a large amount of ferroelectric rhombohedral phase in the MPB region; k_p showed a maximum value between x = 0.25 and 0.3, while d_{33} showed a maximum value at x = 0.30, which is thought to be because the dielectric constant of the x = 0.3 composition is much larger than that of x = 0.25. It has been reported that the dielectric and piezoelectric responses are enhanced in the MPB region because the free energy barrier between ferroelectric phases is low, activating polarization rotation and the movement of domain walls in response to an external electric field [10-12]. Fig. 4 shows that the x = 0.3 composition exhibited moderate piezoelectric properties of d_{33} = 178 pC/N and k_p = 0.357, and a very high Curie temperature of 516°C, which indicates that the composition has a high potential for a high-temperature piezoelectric sensor.

Fig. 5 shows the ferroelectric P-E hysteresis curves obtained by applying an electric field of 6 kV/mm to (1-x)BF-xBT ceramics. Samples with a BT mole fraction of 0.25 or less show P-E hysteresis curves that are not sufficiently saturated, and as x increases to 0.35, the hysteresis curve gradually changes to a saturated shape.

When the BT mole fraction increases to 0.35 or higher, the P-E hysteresis curve gradually becomes thinner and slanted, and the maximum polarization (P_m) and remanent polarization (P_r) continue to decrease. Fig. 5(c) shows the changes in P_m, P_r, and coercive electric field (E_C) with increasing BT mole fraction [10-12,17]. As shown in Fig. 5, P_m and P_r showed very small values in the x = 0.2 composition; as x increased, the two values gradually increased, showing a maximum at x = 0.35, and then decreased. When an electric field of 6 kV/mm was applied to compositions with x = 0.3 or lower, the P-E hysteresis curves could not be sufficiently saturated; the E_C obtained from a saturated hysteresis curve by increasing the magnitude of the applied electric field is shown together as a dotted line in Fig. 5(c). As can be confirmed in Fig. 5(c), the E_C measured in the saturated P-E curve of the x = 0.2 composition showed a very large value of about 7 kV/mm, which indicates that the reason why the P-E hysteresis curve in Fig. 5(a) shows very small polarization is that the coercive field was larger than the magnitude of the applied electric field (6 kV/mm). Fig. 5(c) shows that the E_C continuously decreases

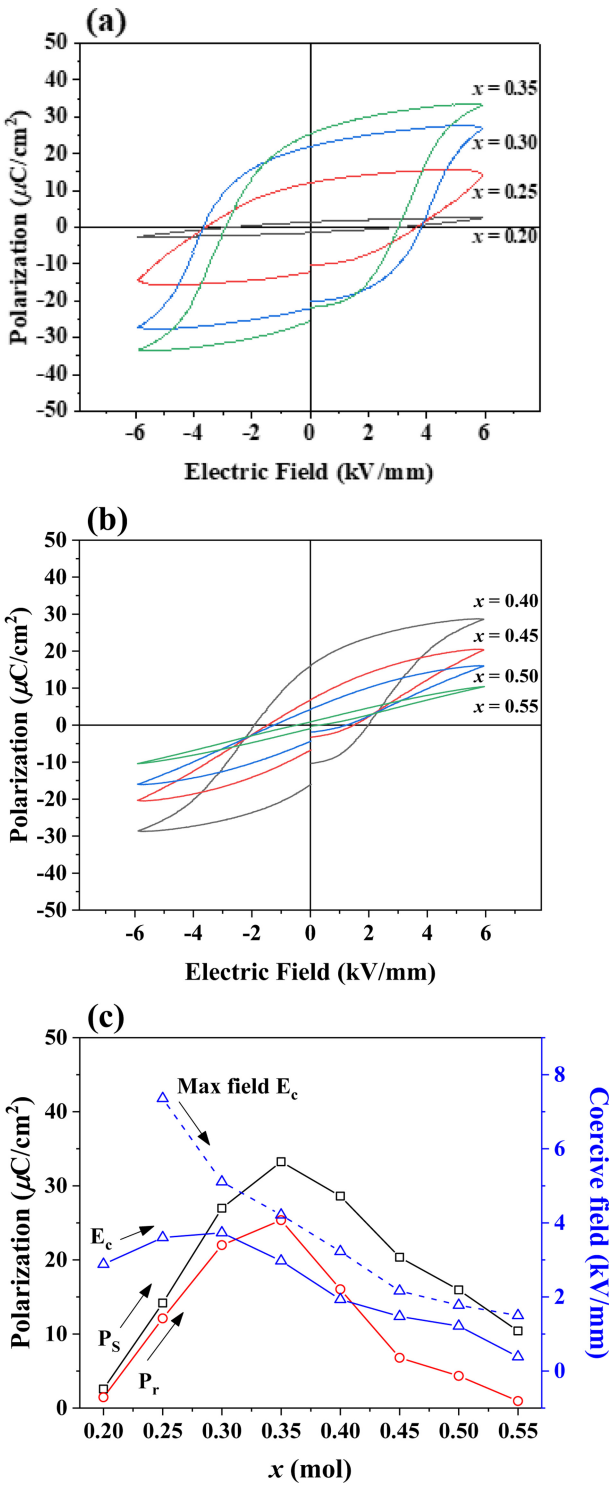

Fig. 5. Ferroelectric P-E hysteresis curves of (1-*x*)BF-*x*BT ceramics with (a) $x = 0.2 – 0.35$ and (b) $x = 0.4 – 0.55$, and (c) changes in P_m, P_r and E_C with the increase of BT mole fraction.

as the BT mole fraction increases. This result suggests that the reason the hysteresis curves of the $x = 0.2–0.3$ compositions were not saturated is that the E_C was so large that an electric field of 6 kV/mm could not induce sufficient polarization reversal. The increase in P_m and P_r as x increased from 0.2 to 0.35 in Fig. 5(c) is thought to be because the ferroelectric domain switching occurred sufficiently due to the decrease in E_C.

In addition, the facilitated polarization rotation and domain wall motion in the MPB region are thought to contribute to the increase in P_m and P_r. When the BT mole fraction increased to 0.35 or higher, P_m and P_r continued to decrease; it is thought that the maximum polarization decreased as the volume fraction of PNRs in the relaxor ferroelectric phase, which is the main phase in this composition range, gradually decreased. The remanent polarization continued to decrease because the ergodic relaxor phase gradually increased. These results are in good agreement with previous reports that when the BT mole fraction increases to 0.35 or higher in BF-BT ceramics, the relaxor phase transition temperature gradually decreases, and the phase transitions from a non- ergodic relaxor state to an ergodic relaxor state [10-12,17]. Figs. 6(a) and (b) show the ferroelectric S-E hysteresis curves measured by applying a bipolar electric field of 6 kV/mm to (1-*x*)BF-*x*BT ceramics and the change in strain with the BT mole fraction. The changes in positive strain (S_{pos}), negative strain (S_{neg}), and total strain (S_{total}) with the BT mole fraction obtained from the bipolar strain curves are shown in Fig. 6(c).

Here, the total strain was defined as the sum of the absolute values of the maximum positive strain and the maximum negative strain. In the case of the $x = 0.2$ composition, as explained previously based on the P-E hysteresis curve, the coercive field was so large that domain switching hardly occurred when an electric field of 6 kV/mm was applied, resulting in a very small strain; in the $x = 0.25$ composition, a typical S-E hysteresis curve of a ferroelectric material, in which the negative strain appears larger than the positive strain, was observed, but it still showed an unsaturated shape [10,17]. When the BT mole fraction increased from 0.25 to 0.35, the negative strain was maintained nearly constant, while the positive strain continuously increased. Accordingly, the total strain also gradually increased, showing the largest value at $x = 0.35$. This is considered to be caused by easier domain switching due to the decrease in the coercive field and the MPB effect. However, when x increased to 0.4, the positive strain increased slightly, but the negative strain decreased significantly, and as a result, the total strain decreased significantly. Generally, in the ergodic relaxor state, it is known that the remanent polarization and negative strain become almost zero because back-switching occurs, in which the electric dipoles of the PNRs return to a disordered state when the electric field is removed [10-12,16,17]. Therefore, it is considered that when the BT mole fraction

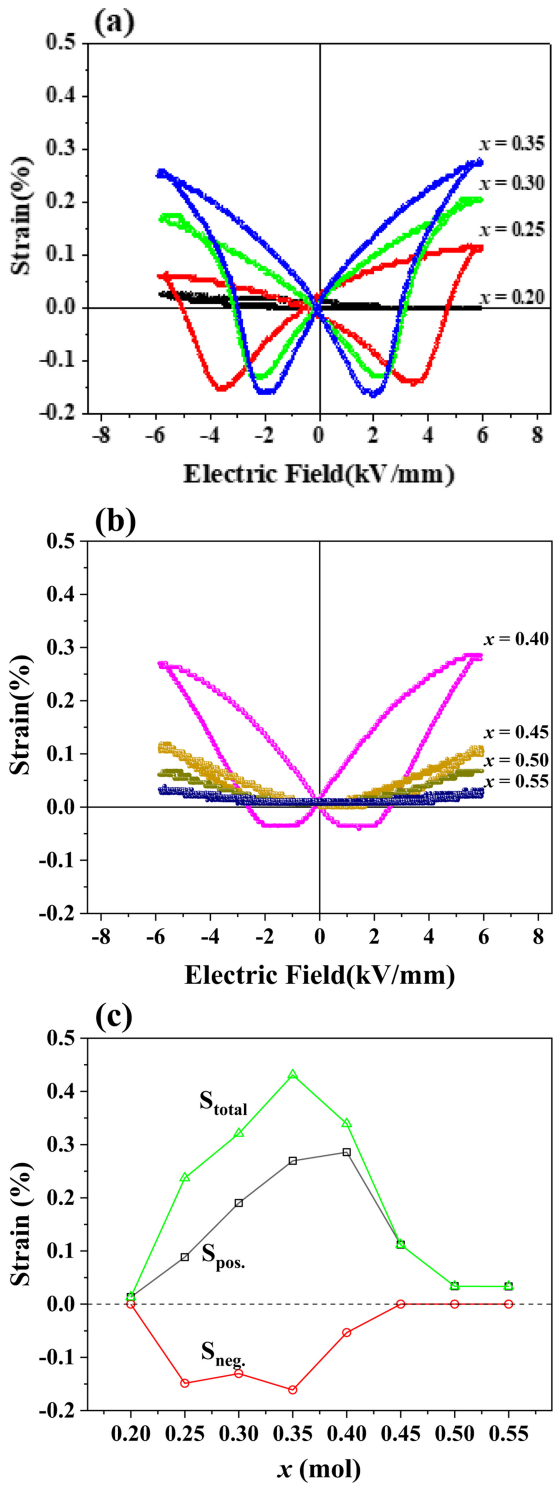

Fig. 6. Bipolar S-E hysteresis curves of (1-*x*)BF-*x*BT ceramics (a) at x = 0.2 – 0.35 and (b) at x = 0.4 – 0.55, and (c) changes in S_{pos}, S_{neg}, and S_{total}, with the increase of BT mole fraction.

increased to 0.4 or higher, the negative strain significantly decreased because the ergodic relaxor phase increased. Furthermore, in the $x \geq 0.4$ range, the overall strain also significantly decreased because the volume fraction of the PNRs continuously decreased as discussed based on the P-E hysteresis curves.

Figs. 7(a) and (b) show S-E hysteresis curves measured by applying a unipolar electric field of 6 kV/mm to (1-*x*)BF-*x*BT ceramics, while Fig. 7(c) shows the maximum strain and strain hysteresis, and Fig. 7(d) shows the piezoelectric strain constant (d_{33}*) calculated from the converse piezoelectric effect. The change in unipolar strain with the BT mole fraction is similar to the change in bipolar strain in Fig. 6, but the unipolar strain showed its maximum at the x = 0.40 composition. Since unipolar strain is defined as the difference between the strain when the electric field is 0 and the strain at the maximum electric field, it generally shows a relatively small value in ferroelectric materials with large remanent strain, and a larger value in relaxor ferroelectrics with almost no remanent strain. As can be seen from Fig. 6, the x = 0.40 composition had a smaller total strain than the x = 0.35 composition because the negative strain significantly decreased, but the positive strain increased; for this reason, the x = 0.40 composition showed a larger unipolar strain. Furthermore, as x increased from 0.2 to 0.4, the strain hysteresis (S_{hys}) increased, which is attributed to the continuous increase in the ratio of the relaxor phase. In the relaxor phase, domain switching or phase transition to a ferroelectric phase occurs above a certain threshold electric field when an external electric field is applied, so the strain appears very small in the low electric field region and then increases rapidly above the threshold electric field. The strain also maintains a higher value when the electric field is removed, resulting in large strain hysteresis. However, when x increased to 0.4 or higher, the overall strain significantly decreased as the volume fraction of the polar regions decreased, and accordingly, the strain hysteresis also significantly decreased. Meanwhile, the piezoelectric strain constant (d_{33}*) also showed the same trend as the unipolar strain. The composition with x = 0.4, showed a large strain of 0.308%, a high d_{33}* of 513 pC/N, and a relatively low strain hysteresis of 0.25%, respectively. This is compared with previously reported results for BF-BT solid solution ceramics in Table 2. As can be seen in Table 2, (1-*x*)BF-*x*BT solid solution ceramics show large piezoelectric strains in the x = 0.35 – 0.4 composition range; the (1-*x*)BF-*x*BT sample with the x = 0.36 composition showed the maximum strain and piezoelectric strain constant, but at the same time, a very large strain hysteresis of 47%. The x = 0.4 composition in this work shows a large strain and a high piezoelectric strain constant, while also showing a low value for strain hysteresis. It is expected that further improved piezoelectric strain characteristics could be obtained when the composition and manufacturing process are finely optimized in the BT mole fraction range of 0.35–0.4.

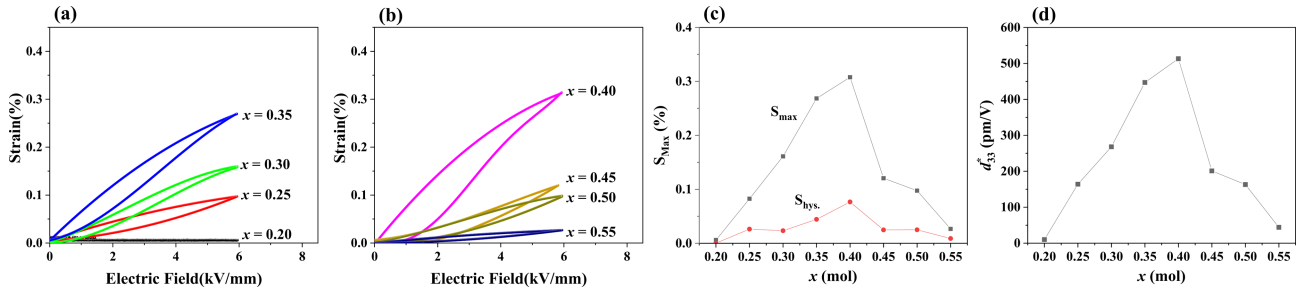

Fig. 7. (a), (b) unipolar S-E curves of (1-*x*)BF-*x*BT ceramics, and (c) S_{max} and S_{hys} and (d) d_{33}^* as a function of the BT mole fraction.

Table 2. Piezoelectric Strain Characteristics in (1-*x*)BF-*x*BT binary solid solution ceramics.

Composition	S_{max} (%)	d_{33}^* (pm/V)	ΔH (%)	E (kV/cm)	Ref.
$0.60BiFeO_3$-$0.40BaTiO_3$	0.210	350	-	60	15
$0.64Bi_{1.02}FeO_3$-$0.36BaTiO_3$	0.380	633	47	60	14
$0.65Bi_{1.02}FeO_3$-$0.35BaTiO_3$	0.202	405	17	50	11
$0.60BiFeO_3$-$0.40BaTiO_3$	0.308	513	25	60	This work

4. CONCLUSIONS

In (1-*x*)BF-*x*BT ceramics, the crystal structure changed from rhombohedral to pseudo-cubic as the BT mole fraction increased from 0.2 to 0.5. In the composition range of 0.25–0.4, the rhombohedral phase and the pseudo-cubic phase coexisted; as the BT mole fraction increased, the fraction of the pseudo-cubic phase increased, and the rhombohedral distortion (90^o-α) decreased. The (1-*x*)BF-*x*BT ceramics with a BT mole fraction of 0.3 or less showed a ferroelectric phase transition, while the samples with x = 0.35 or higher showed relaxor ferroelectric phase transition behavior. The 0.7BF-0.3BT specimen exhibited moderate piezoelectric properties with a piezoelectric charge constant (d_{33}) of 178 pC/N and an electromechanical coupling factor (k_p) of 0.357, along with a high Curie temperature (T_C) of 516^oC, suggesting strong potential for high-temperature piezoelectric sensor applications. The P-E and S-E hysteresis curves showed unsaturated ferroelectric hysteresis in the x = 0.2–0.3 compositions. The largest polarization and strain were observed at a BT mole fraction of 0.35, which is attributed to the low coercive field and the MPB effect. The 0.6BF-0.4BT ceramic showed a maximum unipolar strain of 0.308%, a high d_{33}* of 513 pC/N, and a low strain hysteresis of 0.25%.

CRediT Authorship Contribution Statement

Ye-Rok Choi: Data curation, Formal analysis, Investigation, Methodology, Validation, Visualization. **Chae-Il Cheon:** Conceptualization, Data curation, Formal analysis, Investigation, Methodology, Resources, Supervision, Validation, Visualization, Writing – original draft. **Ki-Woong Chae:** Conceptualization, Funding acquisition, Investigation, Project administration, Resources, Supervision, Writing – review and editing.

Declaration of Competing Interest

The authors declare that they have no known competing financial interests or personal relationships that could have appeared to influence the work reported in this paper.

Acknowledgements

This research was supported by the Academic Research Fund of Hoseo University in 2024 (2024-0161-01).

REFERENCES

[1] W. Jo, R. Dittmer, M. Acosta, J. Zang, C. Groh, E. Sapper, et al., Giant electric-field-induced strains in lead-free ceramics for actuator applications – status and perspective, J. Electroceram. 29 (2012) 71–93.
[2] F. Li, M.J. Cabral, B. Xu, Z. Cheng, E.C. Dickey, J.M. Lebeau, et al., Giant piezoelectricity of Sm-doped $Pb(Mg_{1/3}Nb_{2/3})O_3$ -$PbTiO_3$ single crystals, Science 364 (2019) 264–268.
[3] S.-E. Park, T.R. Shrout, Ultrahigh strain and piezoelectric behavior in relaxor based ferroelectric single crystals, J. Appl. Phys. 82 (1997) 1804–1811.
[4] H. Fu, R.E. Cohen, Polarization rotation mechanism for ultrahigh electromechanical response in single-crystal piezoelectrics, Nature 403 (2000) 281–283.
[5] H.-L. Li, Y. Zhang, J.-J. Zhou, X.-W. Zhang, H. Liu, J.-Z. Fang, Phase structure and electrical properties of *x*PZN–(1−*x*)PZT piezoceramics near the tetragonal/rhombohedral phase boundary, Ceram. Int. 41 (2015) 4822–4828.

[6] G. Xia, Y. Yang, Z. Du, H. Liu, X. Tong, Large strain with broad temperature insensitivity in PZT-PNN multilayer piezoactuators, Ceram. Int. 50 (2024) 18821–18831.
[7] C. Dixon, Restriction of the Use of Certain Hazardous Substances in Electrical and Electronic Equipment (RoHS), Telecom Connections Ltd, Statement, 2019.
[8] J. Chen, F. Luo, Y. Liu, D. Jiang, L. Xing, Z. Li, Enhanced piezoelectric properties in coarse-grained $0.7Bi(Fe_{0.9985}Mn_{0.0015})O_3$-$0.3BaTiO_3$ ceramics, J. Alloys Compd. 960 (2023) 170845.
[9] D. Wang, G. Wang, S. Murakami, Z. Fan, A. Feteira, D. Zhou, et al., $BiFeO_3$ -$BaTiO_3$: A new generation of lead-free electroceramics, J. Adv. Dielectr. 8 (2018) 1830004.
[10] B. Xun, A. Song, J. Yu, Y. Yin, J.-F. Li, B.-P. Zhang, Lead-Free $BiFeO_3$-$BaTiO_3$ Ceramics with High Curie Temperature: Fine Compositional Tuning across the Phase Boundary for High Piezoelectric Charge and Strain Coefficients, ACS Appl. Mater. Interfaces 13 (2021) 4192–4202.
[11] S.O. Leontsev, R.E. Eitel, Dielectric and Piezoelectric Properties in Mn-Modified $(1-x)BiFeO_3-x$ $BaTiO_3$ Ceramics, J. Am. Ceram. Soc. 92 (2009) 2957–2961.
[12] M.H. Lee, D.J. Kim, J.S. Park, S.W. Kim, T.K. Song, M.H. Kim, et al., High-Performance Lead-Free Piezoceramics with High Curie Temperatures, Adv. Mater. 27 (2015) 6976–6982.
[13] L. Luo, N. Jiang, X. Zou, D. Shi, T. Sun, Q. Zheng, et al., Phase transition, piezoelectric, and multiferroic properties of $La(Co_{0.5}$ $Mn_{0.5})O_3$ -modified $BiFeO_3$ -$BaTiO_3$ lead-free ceramics: Properties of LCMO-modified $BiFeO_3$ -$BaTiO_3$ lead-free ceramics, Phys. Status Solidi A 212 (2015) 2012–2022.
[14] D. Wang, Z.Fan, W. Li, D. Zhou, A. Feteira, G. Wang, et al., High Energy Storage Density and Large Strain in $Bi(Zn_{2/3}$ $Nb_{1/3})O_3$-Doped $BiFeO_3$-$BaTiO_3$ Ceramics, ACS Appl. Energy Mater. 1 (2018) 4403–4412.
[15] X. Liu, J. Zhai, B. Shen, Novel bismuth ferrite-based lead-free incipient piezoceramics with high electromechanical response, J. Mater. Chem. C 7 (2019) 5122–5130.
[16] J. Chen, J.E. Daniels, J. Jian, Z. Cheng, J. Cheng, J. Wang, et al., Origin of large electric-field-induced strain in pseudo-cubic BiFeO3–BaTiO3 ceramics, Acta Mater. 197 (2020) 1–9.
[17] C. Li, T. Zheng, J. Wu, Competitive mechanism of temperature-dependent electrical properties in $BiFeO_3$-$BaTiO_3$ ferroelectrics controlled by domain evolution, Acta Mater. 206 (2021) 116601.
[18] H. Qin, J. Zhao, X. Chen, H. Li, S. Wang, Y. Du, et al., Improved piezoelectric properties in $Bi(Mg_{2/3}$ $Nb_{1/3})O_3$ -modified $BiFeO_3$ –$BaTiO_3$ lead-free piezoelectric ceramics, J. Am. Ceram. Soc. 107 (2024) 6833–6843.
[19] N. Zhao, H. Fan, X. Ren, J. Ma, J. Bao, Y. Guo, et al., Dielectric, impedance and piezoelectric properties of $(K_{0.5}Nd_{0.5})TiO_3$-doped $0.67BiFeO_3$-$0.33BaTiO_3$ ceramics, J. Eur. Ceram. Soc. 39 (2019) 4096–4102.
[20] Y. Hao, Y. Yin, H. Liu, X.-X. Zhou, L.-T. Xie, H.-Y. Xu, et al., Optimized strain property in Sm^{3+} doped $0.67BiFeO_3$-$0.33BaTiO_3$ ceramics by electric field induced lattice distortion and domain wall motion, J. Alloys Compd. 1005 (2024) 175791.
[21] Y. Yin, Y. Tang, W. Pan, A. Song, J. Yu, B. Zhang, Relaxor behaviors enhance piezoelectricity in lead-free $BiFeO_3$-$BaTiO_3$ ceramics incorporated with a tiny amount of $Bi(Mg_{1/2}Ti_{1/2})O_3$ near the morphotropic phase boundary, Ceram. Int. 47 (2021) 9486–9494.
[22] F. Li, S. Zhang, D. Damjanovic, L. Chen, T.R. Shrout, Local Structural Heterogeneity and Electromechanical Responses of Ferroelectrics: Learning from Relaxor Ferroelectrics, Adv. Funct. Mater. 28 (2018) 1801504.